water

MDPI

Article

Elemental Fractionation in Sabellariidae (Polychaeta) Biocement and Comparison with Seawater Pattern: A New Environmental Proxy in a High-Biodiversity Ecosystem?

Claudia Deias [1], Adriano Guido [2,*], Rossana Sanfilippo [1], Carmine Apollaro [2], Rocco Dominici [2], Mara Cipriani [2], Donatella Barca [2] and Giovanni Vespasiano [2]

[1] Department of Biological, Geological and Environmental Sciences (DipBioGeo), University of Catania, Corso Italia 57, 95129 Catania, Italy; claudia.deias@phd.unict.it (C.D.); sanfiros@unict.it (R.S.)
[2] Department of Biology, Ecology and Earth Sciences (DiBEST), University of Calabria, Via Ponte Bucci 4, Cubo 15B, 87036 Rende, Italy; carmine.apollaro@unical.it (C.A.); rocco.dominici@unical.it (R.D.); mara.cipriani@unical.it (M.C.); donatella.barca@unical.it (D.B.); giovanni.vespasiano@unical.it (G.V.)
* Correspondence: adriano.guido@unical.it; Tel.: +39-84-493651

Abstract: The polychaete worm *Sabellaria alveolata* builds shallow-water aggregates of tubes by agglutinating sands using a secreted glue. Sabellarid bioconstructions represent fragile and dynamic habitats that host numerous associated organisms, playing a key ecological role. A two-year study on bioconstructions from three Sicilian sites (Simeto, Portopalo, and Falconara) investigated the balance between reef status and environmental parameters through a geochemical comparison of biocement tube portions and the surrounding waters. Water pollution by heavy metals, which is monitored in marine waters, is a result of river, domestic, and industrial discharges. The major constituents from the biocements of the three sites showed concentrations comparable to those in the seawater, while trace elements (Cr, Ni, Cu, Zn, and As) showed concentrations significantly higher than the mean seawater composition. These similar trends confirm a close dependence between the presence of trace elements (metals) in the seawater and the subsequent bioaccumulation in the biocement produced by the worm. The results also showed that Ca and Mg are fractionated by biocement independent of their water concentrations, in contrast to the trace elements. Further studies addressing the biomineralization processes and the relative fractionation of trace elements in *Sabellaria* biocement will allow it to be validated as a valuable proxy for short- and long-term environmental studies.

Keywords: *Sabellaria alveolata*; agglutinated tubes; biomineralization; trace elements; geochemistry; seawater composition; environmental pollution; Mediterranean Sea

Citation: Deias, C.; Guido, A.; Sanfilippo, R.; Apollaro, C.; Dominici, R.; Cipriani, M.; Barca, D.; Vespasiano, G. Elemental Fractionation in Sabellariidae (Polychaeta) Biocement and Comparison with Seawater Pattern: A New Environmental Proxy in a High-Biodiversity Ecosystem? *Water* **2023**, *15*, 1549. https://doi.org/10.3390/w15081549

Academic Editor: Jun Yang

Received: 17 March 2023
Revised: 6 April 2023
Accepted: 11 April 2023
Published: 14 April 2023

1. Introduction

Sabellaria alveolata [1] is a gregarious polychaete sabellariid that lives in tubes of sediment agglutinated using a particular proteinaceous glue secreted by specialized glands [2–5]. The species forms bioconstructions in mesolittoral–upper infralittoral bottoms dominated by high hydrodynamic energy, where it captures suspended sand grains to build its aggregated tubes [6–9].

S. alveolata is distributed in the temperate eastern Atlantic, from Morocco to the northern coasts of the British Islands [7,10–17], with the largest reefs mainly developed on the British [18] and French coasts [8,15,19,20]. The species is also present in the western Mediterranean. In particular, it is most common on the Tyrrhenian Italian coasts [9,21,22] and the southern Sicilian coasts (Strait of Sicily) [23–28].

Like all Sabellariidae, *Sabellaria* builds bioconstructions up to 1 m high and hundreds of square meters wide, thus modifying the morphology of substrates, stabilizing beach sediments, and protecting the coast from wave action [29–31]. They are ephemeral structures

subject to physical damage caused by meteorological events such as extreme storms [32,33], which can cause their severe reduction or disappearance in a very short time [7]. However, *Sabellaria* is capable of constructing tubes to repair small damaged areas of bioconstruction within a few weeks or months [11,34,35], but heavier impacts may take years to decades to repair [16].

Sabellaria bioconstructions play a very important ecological role since they represent a habitat that hosts a great variety of benthic organisms, thus enhancing biodiversity on the sea bottom where they are found [13,26,36].

The functional role played by sabellariid reefs and the diverse and severe threats they are subjected to make them valuable and vulnerable marine habitats. For this reason, they are considered by European Union (EU) legislation to be priority habitats and are included in the Habitats Directive (Directive 92/43/EEC) and the European Red List of Habitats [37].

Coastal ecosystems are highly impacted by humans and represent the end points of many substances released by human activities [38], including toxic metal contaminants from agricultural, industrial, and urban activities [39]. Although polychaetes have frequently been used as a representative group to assess the health of benthic ecosystems and to analyze the effects of pollutants in the water column and in sediments [40–47], very few studies are known for Sabellariid worms, particularly on trace metals found in their soft bodies [48–50]. To date, no studies have investigated the presence of trace elements in the biocement of their tubes and possible correlations of the composition of these biopolymers with the chemistry of the surrounding seawaters. The biocement has solely been investigated in terms of the composition, structure, and distribution of the agglutinated grains [2,3,8,51–53], except for in Pacific *Phragmatopoma californica*, whose technique of gluing has been investigated [5,54–59]. The biocement is composed of proteins and divalent cations, and it provides the adhesion of the sandy elements of the tube, which rapidly solidify after contact with seawater [56].

In the past decades, the biomineralization processes and the chemical relationship between the elemental concentrations of biominerals and environmental water have been extensively investigated. These studies revealed surprising information on the relationships between metal contents, some physico-chemical parameters of seawater, and the occurrence of abnormalities in the organisms [50,60–67]. Research has been based on the soft tissues of recent organisms (i.e., bivalves, mollusks, fishes, and green and red algae) [68–73] and on fossilized hard tissues [69,74–76]. Indeed, major, minor, and trace constituents are incorporated into the soft and hard tissues of organisms directly from seawater, reflecting the seawater's composition, the physical conditions, and the biological control during their growth.

This evidence has not been investigated in Sabellariid biocement. Therefore, this study aimed to be the first attempt to investigate whether the composition of biocement can mirror that of the environmental water. For this purpose, portions of *S. alveolata* bioconstructions and water samples in their surroundings were collected at three coastal sites in eastern and southern Sicily in order to (a) estimate the quantitative concentrations of various elements on selected spots on tubes of biocement of *S. alveolata* from the three investigated sites; (b) assess and compare the chemical compositions of the environmental waters; (c) compare data from the biocement and the water; and (d) evaluate whether the fractionation of biocement elements was in equilibrium with the water solution in order to detect possible new biological proxies that are useful for environmental monitoring and the reconstruction of past geochemical seawater conditions.

2. Study Areas

The study areas were located in the western Mediterranean Sea along the southeastern Sicilian coast (Figure 1a,b). One of the three sampling sites was placed on the Ionian coast (Simeto mouth: Figure 1c), while the other two were located on the coast of the Strait of Sicily (Portopalo: Figure 1d; Falconara: Figure 1e). Although the three sites were different geomorphologically, they all neighbored a sandy beach (Figure 1c–e). A wide shelf with

shallow bottoms is typical of the southern Sicilian side [77], while a very narrow shelf with a rocky and steep seafloor occurs along the Ionian coast. The Simeto mouth area, however, compared to the rest of the Ionian coast, has extended soft bottoms due to an abundant sediment load [78].

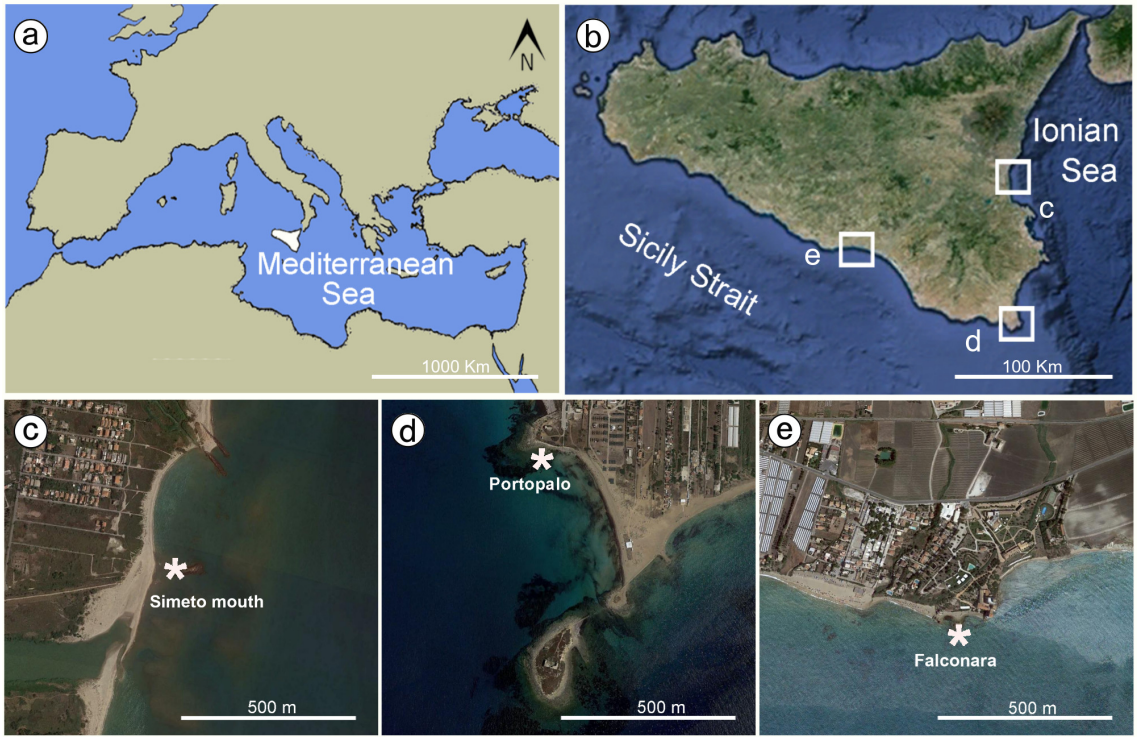

Figure 1. (**a**,**b**) Study areas (white squares) in the Mediterranean Sea, with the locations of the *S. alveolata* on the Sicilian coasts: (**c**) Simeto mouth, (**d**) Portopalo, and (**e**) Falconara. The maps (**c**–**e**) are from Google Earth. Asterisks indicate sampling sites.

Simeto (37°24′11.4″ N; 15°05′30.3″ E). This site included a sandy beach in front of the Simeto mouth, the greatest watercourse of Sicily, running from the Nebrodi Mountains, and the smaller San Leonardo River, running from the Hyblean Plateau [79,80]. The mouth, together with the nearby wetlands (humid areas), is an area of strong naturalist importance in terms of the geomorphological, faunal, and floristic aspects. It has been protected, from a naturalistic point of view, since it was established as an oriented nature reserve in 1984.

The area is a delta coast that is currently formed by a very narrow beach of coarse-to-fine sands. Discontinuous levels of recent terraced fluvial sands and silts crop out together with sandy beach deposits. More inland, they overlay Pliocene calcarenites and clays and Holocene alluvial sands and clays. The human-induced changes in the equilibrium regulating the sediment supply to the coast during the last century in the high part of the Simeto drainage basin caused strong erosion with marked coastal land loss.

In this area, strong coastal erosion has occurred for several years [80]. The beach has a high receding rate due to the decrease in the sediment supply and the consequent erosional wave action along the coast. This exposed the oldest sandy levels of the beach, removing the primary cover of the modern beach. Locally, the strong erosive action of the waves and river have exhumed the lower indurated levels of the beach, consisting of discontinuous levels of cemented sandy deposits (beach rocks) [78].

The bottom in front of the shoreline is sandy–muddy and slopes very weakly offshore, with a depth of 1 m about 50 m from the coast. A natural islet with yellow Pliocene sands at its base largely surrounded by large breakwaters occurs ca. 80 m offshore. Sabellaria bioconstructions (Figure 2a) are distributed along a submerged sandy curb connecting the coast to the islet at depths from 45 m to 60–70 m, and they have pillow-like morphologies [25].

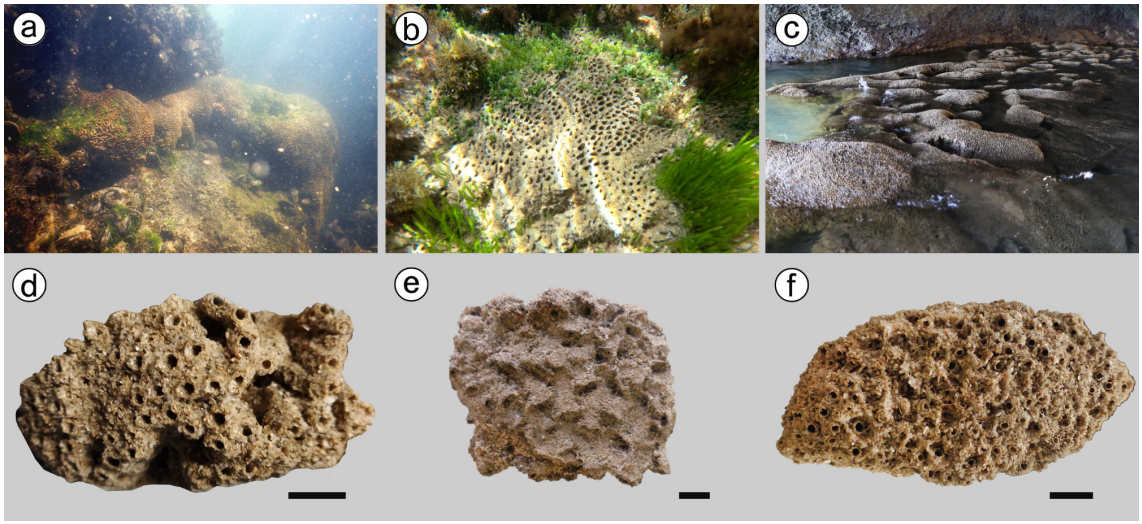

Figure 2. Bioconstructions of *S. alveolata* at the three Sicilian sites and related sampled portions: (**a**,**d**) pillow-like morphology (Simeto), (**b**,**e**) crust-like morphology (Portopalo), (**c**,**f**) bank-like morphology (Falconara). Scale bars: 1 cm.

Portopalo di Capo Passero (36°39′3.9″ N, 15°4′37.6″ E). The site was in a sub-flat rocky area with sparse vegetation and numerous greenhouses. The coast consists of a rocky headland bordering a wide beach to the east. The outcropping rock includes Miocene limestones of the Climiti Mounts Formation with the Melilli Member given by whitish calcarenites and calcilutites with microfauna (Burdigalian–Serravallian) locally overlaid by Upper Pleistocene to Holocene dunes and modern beach deposits [81]. The rocky bottom slopes very weakly offshore, with a depth of 1.5 m at about 50 m from the coast, and shows a dense algal cover and thin discontinuous deposits of organogenic sands [82]. The *S. alveolata* bioconstructions (Figure 2b) are distributed immediately east of the rocky headland, from 1 m to 7 m of depth, and have a crust-like morphology [82].

Falconara (37°06′28.1″ N, 14°03′06.9″ E). The site was in the Gulf of Gela, within a coastal area that is a Natura 2000 site and a site of community importance (S.C.I.) due to the presence of rare and threatened species and natural habitats such as dune ridges. The entire coastal area is subject to retreat due to strong exposure to wave motion and the presence of tourist complexes and greenhouse-crop systems that have occupied the spaces between the ancient dune cordons [83,84]. The Salso River and three torrents flow within this area, but they pass through predominantly evaporite rocks (mainly gypsum), resulting in high-solute but low-sediment loads [85]. Geologically, the rock outcrops are Lower Pliocene marls (Trubi). In addition, brecciate limestone (base limestone) and grey-white laminate limestones crop out. They are overlaid by Middle–Late Pleistocene marine terrace deposits consisting of brown-yellow-colored sands with elongated quartzarenite pebbles. Recent aeolian sands and dune and beach sands are the present-day deposits [77]. The area comprises a narrow sandy beach delimited eastward by the Falconara Castle promontory that projects offshore for a few meters where a large rock (13 × 23 m) is located. It is articulated and jagged and has a tunnel perpendicular to the coast with a vault about 2 m high. Sabellaria bioconstructions are located within the tunnel and locally around the rock itself, 4 m away from the shoreline. The bioconstructions have a bank-like morphology (Figure 2c).

3. Materials and Methods

Samples from *S. alveolata* bioconstructions were collected from autumn 2020 to autumn 2022 at three different sites on the Sicilian coasts (Figure 1): Simeto, at 45 m from the coastline and a 40 cm depth; Capo Passero, at 1 m from the coastline and a 30 cm depth; and Falconara, at 4 m from the coastline and a 60 cm depth.

For each site, a non-invasive method of sampling very small portions of bioconstructions was performed using gloves, a small hammer, and a chisel. The samples were stored in zip bags and transported to the Laboratory of Palaeontology and Palaeoecology of the Department of Biological, Geological and Environmental Sciences (University of Catania), where they were gently washed under fresh water and air-dried.

Small fragments of the tubes were studied using an optical microscope (Zeiss Axioplan II Imaging, Oberkochen, Germany) at up to 40× magnification. After reflected light characterization, the samples were used for scanning electron microscope (SEM) observations and electron probe microanalyzer (EMPA) microanalyses. The samples were carbon-coated for the EPMA microanalyses and gold-coated for the SEM morphological study. The SEM apparatus was an FEI Philips ESEM-FEG Quanta 200 F operating at 15 kV with a working distance between 10 and 15 µm. The EMPA was a JEOL—JXA 8230 operating at 15 kV with a probe current of 10 nA, a working distance of 11 mm, a take-off angle of 40°, and a live time of 50 s.

The seawater near the sampled bioconstructions was collected from the three sites four times (in duplicate) in September/October 2020, April/May 2021, July 2021, and October 2021. To make the data processing and the interpretation as complete and exhaustive as possible, the seawater analyzed in this work was compared with the world mean composition proposed in previous investigations [86,87].

Physico-chemical parameters, including temperature, pH, Eh, and electrical conductivity, were measured in the field using portable instruments. Three pH buffers with nominal pH values of 4.01, 7.01, and 10.01 at 25 °C were used for pH calibration at each sampling site [88,89].

The total alkalinity was determined via acidimetric titration, using 0.05 N HCl as a titrating agent and methyl orange as an indicator [90,91].

Water samples were filtered in situ through a membrane with a 0.4 µm pore size. Samples for the determination of anions were stored without additional treatments, whereas samples for the determination of cations and trace constituents were acidified after filtration via the addition of suprapure acid (1% HNO_3). All the samples were stored in polyethylene bottles (previously washed in dilute HNO_3 and rinsed with Milli-Q demineralized water) and were kept in cold (4 °C) and dark conditions before the analyses. The concentrations of F^-, Cl^-, Br^-, SO_4^{2-}, NO_3^-, PO_4^{3-}, Na^+, K^+, Mg^{2+}, and Ca^{2+} were determined using HPLC (DIONEX ICS-1100, Sunnyvale, CA, USA). Trace elements were analyzed using a quadrupole inductively coupled plasma-mass spectrometer (ICP-MS, Perkin Elmer/SCIEX, Elan DRCe, Waltham, MA, USA) with a collision reaction cell capable of reducing or avoiding the formation of polyatomic spectral interferences.

The data quality of the major components was evaluated using the charge balance, which was within ±5% for all samples. The precision and accuracy for the minor and trace elements was checked against the NIST1643f standard reference solution. Deviations from the certified concentrations were lower than 5% for all samples. All chemical data were determined in the laboratory of the DiBEST of the University of Calabria and are reported in Tables 1 and 2.

4. Results and Discussion

4.1. Biocement: Morphological and Chemical Analysis

In the agglutinated tubes of the three sampled bioconstructions, the analyzed biocement was spread above the sandy elements with small glue spots that were yellowish to light brown in color, sub-millimeter in size, and barely or not at all detectable by the naked eye (Figure 3a–c).

Particles constituting the tube wall adhere to each other and are held together by droplets or strips of biocement. Small spots of glue fix sub-spherical grains to each other, and adhesion points often show meniscus shapes, which mold the local morphology of grains, when they detach (Figure 3c). Conversely, relatively squat grains and flat fragments with straight edges are fixed to each other with continuous strips of glue that suture their edges. The distribution pattern of glue spots was the same in all observed samples, whereas

there were slight differences in their sizes and especially their abundances on individual sediment elements. Glue spots were, on average, smaller in diameter in the Simeto samples (ca. 60 µm) and larger in Portopalo (ca. 100 µm) (Figure 3d–f). Glue strips had, on average, slightly shorter lengths at Falconara (ca. 170 µm) than at Portopalo and Simeto (ca. 200 µm). Biocement was more abundant among the elements in the Portopalo and Simeto tubes, while it was less present in the Falconara tubes. In fact, individual grains had, on average, more glue spots at Portopalo (8) and Simeto (6) and very few glue spots at Falconara (3–4).

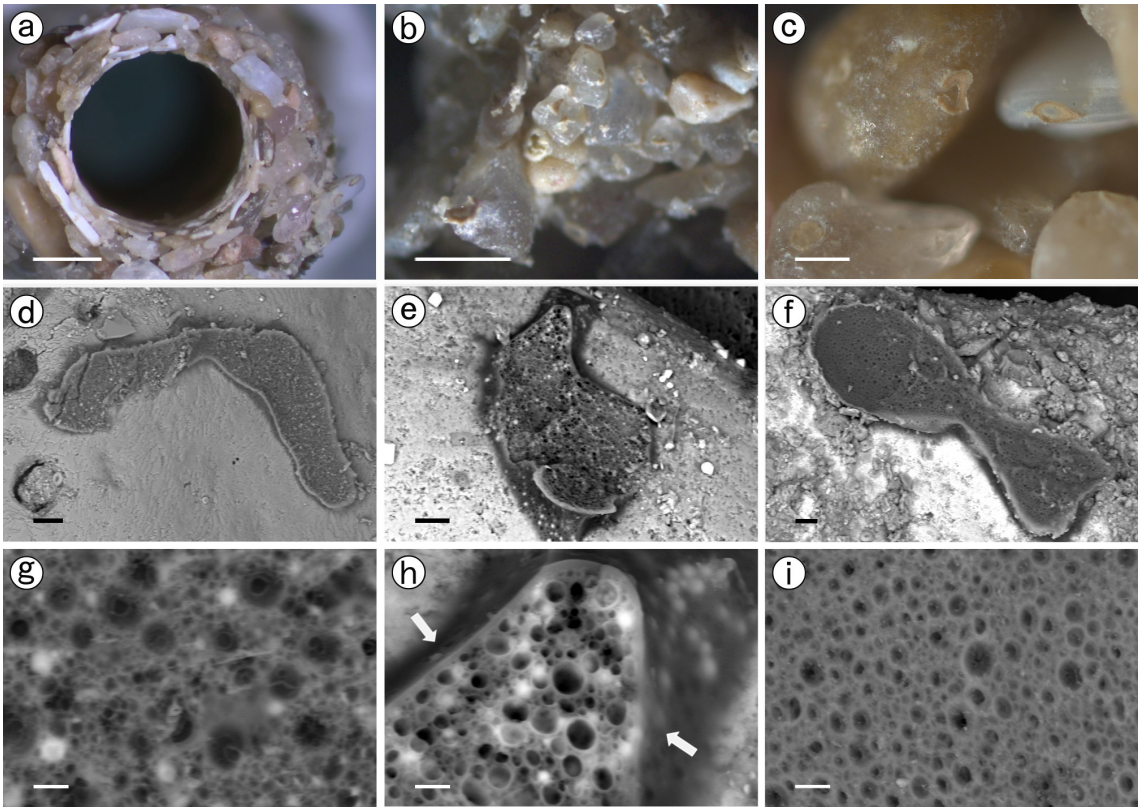

Figure 3. (**a**) Apertural edge of an *S. alveolata* tube with obvious brown spots of biocement on some grains (Simeto); (**b**) detail of a tube wall with numerous biocement portions on sandy elements; (**c**) sand grains with biocement spots showing meniscus surfaces as they mold the morphology of the adjacent detached grains; SEM images of single biocement portions and related internal vacuolar structures from Portopalo (**d**,**g**), Simeto (**e**,**h**), and Falconara (**f**,**i**). The outer surface (white arrows) is indicated in (**h**). Scale bars: (**a**) 1 mm; (**b**) 500 µm; (**c**) 200 µm; (**d**) 20 µm; (**e**,**f**) 10 µm; (**g**–**i**) 2 µm.

The biocement appeared as a solid foam, showing numerous spherical 0.2–10 µm wide pores or bubbles. It revealed comparable foam-like textures, regardless of the position along the tube. Bubbles had a homogeneous organization and distribution (Figure 3g–i). Both biocement spots and strings were thicker (ca. 20 µm) along their outer margins and became thinner (<1 µm) at the contact points of the grains. The major elements consistently observed in the cement from the three sites were C, N, O, Na, Mg, P, S, Cl, K, and Ca (Table 1). Furthermore, some traces of Al, Si, and Fe were found, which could have been unrelated to biocement but related to the influence that the substrate has on it. The variation in the concentrations of the elements was due to the uneven thickness and morphology of the grains and cements. Na and Cl derive from small salt crystals mineralized among the cells of the glue, whereas other elements are localized within the organic biomolecules of the biocement: Mg, Ca, and K are most likely complexed to the cement, while P and N are likely part of the covalent structure of the biocement rather than elements that are complexed to the cement. Sulfur was analyzed in small amounts only at some points inside the biocement. Its concentration never exceeded 1.06 wt%. The concentration of C was

higher in the biocement (average of 44.69 wt%) than in the carbonate substrates, despite the uniform graphite coating of the samples, proving the organic nature of the glue.

Table 1. Average chemical compositions (weight percentage—wt%) of the analyzed biocement from the Portopalo, Simeto, and Falconara samples.

	C	N	O	Na	Mg	Al	Si	P	S	Cl	K	Ca	Fe
	wt%	wt%	wt%	wt%	wt%	wt%	wt%	wt%	wt%	wt%	wt%	wt%	wt%
Portopalo	42.80	12.18	21.70	3.25	3.10	0.26	0.38	2.86	0.80	4.90	0.20	7.12	0.06
Simeto	44.70	13.08	22.14	1.52	3.22	0.11	0.31	6.34	0.79	2.79	0.12	4.70	0.02
Falconara	38.31	10.97	28.62	1.95	1.99	1.41	3.08	4.03	0.66	2.17	0.27	5.46	0.74

The trace elements present in the analyzed biocement from all three sites were B, U, Sr, Zn, Ni, Cu, and Cr (Table 2). There were slight differences in the average percentages: (a) the Portopalo biocement had the highest mass percentages of Zn (average of 0.018 wt%), U (average of 0.038 wt%), and Ni (average of 0.012 wt%); (b) the Simeto biocement had the highest mass percentages of Cu (average of 0.010 wt%) and Sr (average of 0.018 wt%); and (c) the Falconara biocement had the highest mass percentages of B (average of 0.308 wt%) and Cr (average of 0.005 wt%).

Table 2. Averages of the mass percentages of the trace elements in the biocement sampled in summer 2021 at the three sites.

	B	Sr	Cu	Zn	U	Cr	Ni
	wt%	wt%	wt%	wt%	wt%	wt%	wt%
Portopalo	0.299	0.016	0.006	0.018	0.038	0.002	0.012
Simeto	0.103	0.018	0.010	0.014	0.023	0.004	0.003
Falconara	0.308	0.011	0.009	0.008	0.010	0.005	0.011

4.2. Local Seawater Composition and Comparison with Biocement

The mean seasonal physico-chemical seawater parameters (pH, electrical conductivity (EC), and temperature) for each site are summarized in Table 3. Falconara, Portopalo, and Simeto showed comparable mean values, with temperature ranges between 19.4 °C and 28.1 °C, pH values from 8.2 to 8.5, and EC values in a range between 41.3 mS cm^{-1} and 57.8 mS cm^{-1}. As expected, samples collected in the summer period showed the highest temperature values. On the other hand, the pH and EC values did not exhibit correlations with specific seasons.

Table 3. Physico-chemical parameters and concentrations of major components of seawater sampled at the Portopalo, Simeto, and Falconara sites. HCO_3 represents alkalinity in mg of HCO_3 L^{-1}. Each seasonal value represents the average of the two samples that were collected. n.d.= not detected.

ID	Sampling Period	T	pH	EC	Ca	Mg	K	Na	Cl	SO_4	HCO_3	F^-	Br
		°C		mS/cm	mg L^{-1}	mg L^{-1}	mg L^{-1}	mg L^{-1}	mg L^{-1}	mg L^{-1}	mg L^{-1}	mg L^{-1}	mg L^{-1}
Falconara	**Autumn 2020**	24.1	8.4	56.9	618.5	1119.0	337.0	9046.9	21,766.9	2602.1	151.8	12.8	67.3
Falconara	**Spring 2021**	24.1	8.2	44.6	521.4	1506.1	490.8	11,721.3	21,712.1	2465.4	158.6	14.1	64.6
Falconara	**Summer 2021**	25.5	8.2	44.9	585.8	1504.9	441.5	12,419.4	26,157.9	2772.6	183.1	25.5	68.7
Falconara	**Autumn 2021**	19.4	8.3	47.1	646.7	1471.0	479.2	11,761.7	21,629.7	2652.8	158.6	n.d.	59.4
Portopalo	**Autumn 2020**	26.9	8.5	57.8	571.2	1133.9	351.2	9534.9	21,985.2	2623.8	154.1	8.9	70.9
Portopalo	**Spring 2021**	22.9	8.3	45.1	842.4	1585.1	512.0	11,701.5	21,293.4	2675.6	122.0	13.4	71.7
Portopalo	**Summer 2021**	27.2	8.3	45.9	649.6	1548.8	448.0	12,742.9	27,273.1	2723.8	198.3	13.2	64.9
Portopalo	**Autumn 2021**	22.7	8.2	47.3	587.4	1487.2	451.8	12,052.2	24,159.0	2610.3	146.4	11.0	66.0
Simeto	**Autumn 2020**	23.0	8.3	57.1	631.6	1145.3	350.5	8963.3	21,492.8	2622.4	157.1	11.4	63.8
Simeto	**Spring 2021**	22.1	8.2	41.3	759.6	1438.2	467.1	10,944.5	19,631.3	2067.4	183.1	20.7	63.0
Simeto	**Summer 2021**	28.1	8.2	43.3	605.8	1453.4	416.7	12,096.1	25,313.1	2647.6	225.8	16.2	68.5
Simeto	**Autumn 2021**	22.8	8.2	45.2	832.2	1406.8	413.7	11,558.5	23,082.0	2443.5	173.9	14.5	61.3

The concentrations of the major and trace chemical components of seawater are shown in Tables 3 and 4. Overall, samples collected during the summer season showed the highest average values. This trend was mainly recognizable for elements such as Na (>12,000 ppm) and Cl (>25,000 ppm), which showed the lowest values in autumn and spring, respectively. A high concentration reflects the most intense evaporative effects and the reduced input of fresh water from the main rivers during the prolonged summer period. Calcium increases were recorded for the Portopalo and Simeto sites, mainly in the spring period, in contrast to Falconara, where the lowest values were found.

Table 4. Concentrations of trace chemical components of seawater sampled at the Falconara, Portopalo, and Simeto sites. Each seasonal value represents the average of the two samples that were collected.

ID	Sampling Period	Li	B	Cr	Ni	Cu	Zn	As	Se	Rb	Sr	Ti
		μg L^{-1}	μg L^{-1}	μg L^{-1}	μg L^{-1}	μg L^{-1}	μg L^{-1}	μg L^{-1}	μg L^{-1}	μg L^{-1}	μg L^{-1}	μg L^{-1}
Falconara	**Autumn 2020**	227.9	5980.4	109.9	24.1	51.2	345.5	117.4	701.4	132.2	9153.2	672.8
Falconara	**Spring 2021**	210.0	5989.4	75.4	27.1	54.9	332.6	69.1	734.6	136.9	9194.9	653.2
Falconara	**Summer 2021**	210.1	6063.6	101.1	35.0	64.1	269.9	75.0	775.8	128.5	9466.0	635.5
Falconara	**Autumn 2021**	191.3	6020.3	25.8	90.3	216.9	623.9	48.4	346.0	133.2	9144.3	674.7
Portopalo	**Autumn 2020**	222.0	6066.1	106.3	31.9	50.8	385.3	97.9	718.7	141.0	9393.2	700.1
Portopalo	**Spring 2021**	217.9	6048.7	97.6	24.9	56.8	421.2	91.3	718.6	133.4	9567.5	685.5
Portopalo	**Summer 2021**	223.1	6327.6	87.2	31.1	62.9	325.8	81.9	791.8	138.1	9635.5	671.8
Portopalo	**Autumn 2021**	201.2	8038.4	65.0	137.2	268.9	8090.7	54.2	361.6	120.7	8701.2	688.1
Simeto	**Autumn 2020**	216.1	6181.1	94.4	23.3	55.9	271.7	86.1	722.4	134.7	9321.8	675.5
Simeto	**Spring 2021**	192.8	5381.4	78.6	23.8	48.7	289.5	76.7	694.5	117.8	8420.3	603.1
Simeto	**Summer 2021**	223.9	6525.2	108.2	29.5	59.0	291.7	70.9	681.9	130.8	9260.7	615.5
Simeto	**Autumn 2021**	187.6	6954.8	23.8	74.9	270.3	7508.9	50.7	307.2	112.9	8236.4	600.3

Sulphate did not show a trend but had a clear decrease during spring. In this latter case, secondary processes, such as the bacterial reduction of sulphate ([89–92] and references therein), probably mask any possible trend linked to dilution processes.

The Ca/(Ca + Mg) ratio was calculated for both the biocement and the average values (all seasons) of the three seawater samples (Figure 4). Seawater collected in Portopalo, Simeto, and Falconara showed slightly different ratios of 0.32, 0.34, and 0.30, respectively. On the other hand, the Ca/(Ca + Mg) ratios of the three biocements showed an opposite trend from that found in seawater, with values of 0.70, 0.59, and 0.73 for the Portopalo, Simeto, and Falconara biocements, respectively (Figure 4). The opposite trend confirmed that the fractionation of such elements during the formation of biocement is independent of the seawater composition in terms of the major constituents.

Regarding the minor and trace constituents, Sr and B showed the highest concentrations of the entire set of elements, with mean values of ~9000 mg L^{-1} and ~6000 mg L^{-1}, respectively. Sr and Se showed trends comparable to those identified for the major elements (e.g., Na and K), with maximum average values in summer for all three sampling sites. B and Zn showed significantly higher values in autumn 2021 in Portopalo and Simeto. This trend also characterized the Ni and Cu concentrations at all three sites. The anomalous concentrations recognized for the three transition metals (Ni, Cu, and Zn) were probably attributable to local anthropogenic contamination processes due to their proximity to disused or still active industrial areas. For the other trace elements, no trends were evident.

To detect any anomalies from the expected composition of average seawater, the absolute concentrations were normalized to the mean seawater concentration (data from [87]).

By normalizing the mean values of the pH and major constituents with those of average seawater, they were comparable to each other (Figure 5) except for calcium and bicarbonate, while Cl and SO_4 were somewhat comparable. The concentrations of Ca and HCO_3 are controlled by calcite dissolution/precipitation processes, while Cl and SO_4 are probably affected by dilution/evaporation and bacterial reduction processes, respectively. B, Cr, Ni, Cu, Zn, and As showed much higher concentrations than the average seawater

by up to three orders of magnitude. These anomalies were found in all sampling periods. The values were variable, but they were always much higher than the expected averages.

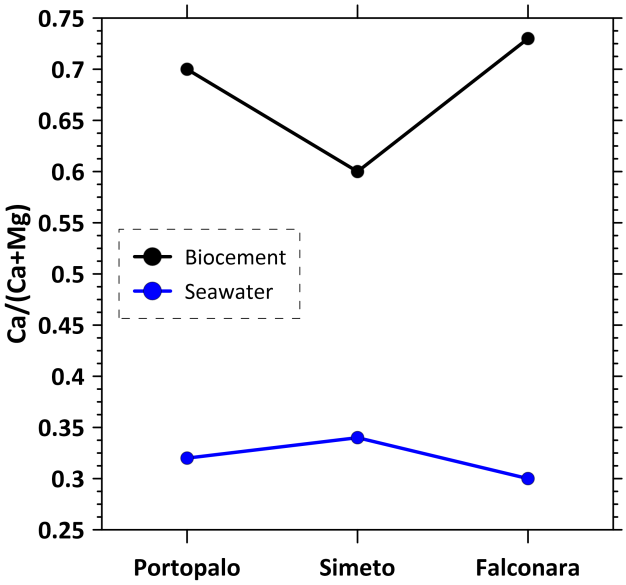

Figure 4. Comparison of the Ca/(Ca + Mg) ratios between the sabellariid biocement and the seawater close to the bioconstructions of the three sites. Note the inverse trend of the concentrations of Ca and Mg between the biocement and the seawater.

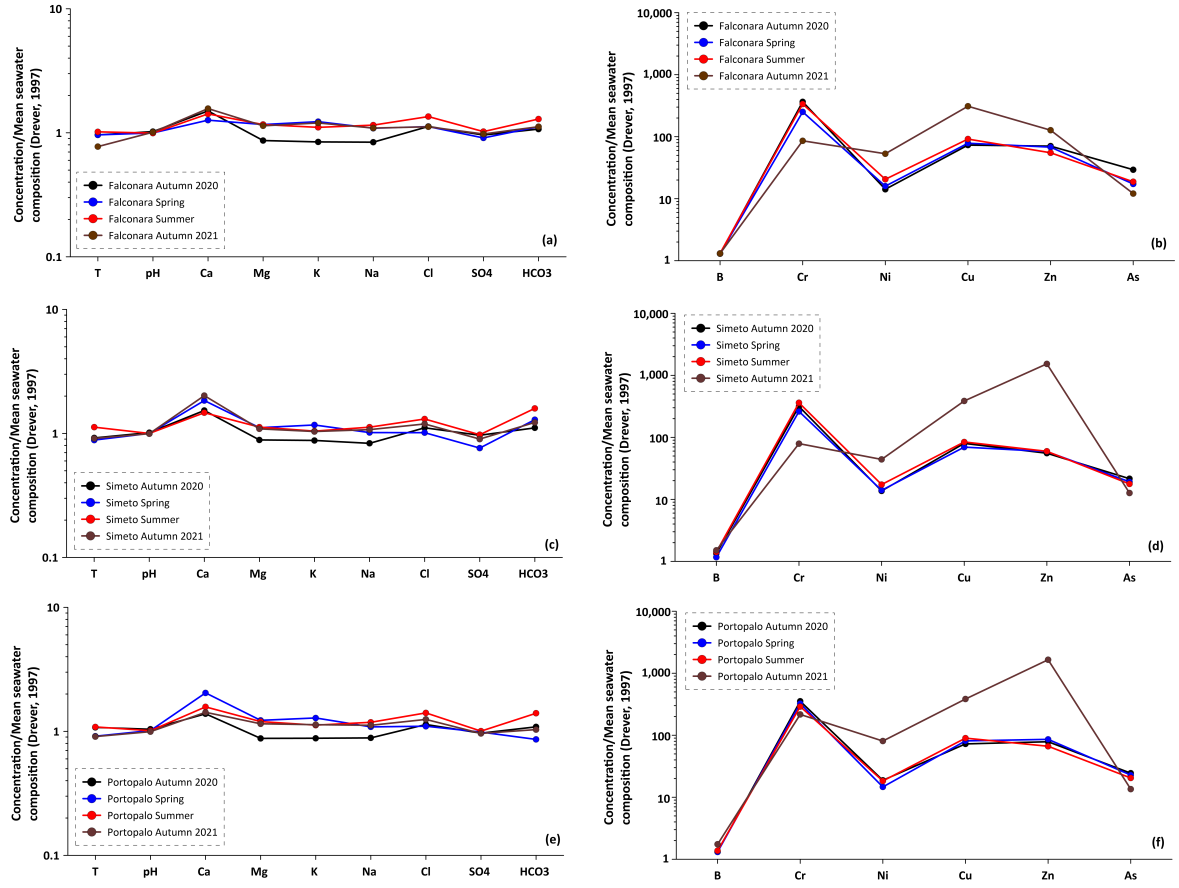

Figure 5. Mean seawater-normalized diagrams (data from [87]) of the physico-chemical parameters and major and trace constituents of samples collected at the Falconara (**a**,**b**), Simeto (**c**,**d**), and Portopalo (**e**,**f**) sites during Autumn 2021, Spring 2022, Summer 2022, and Autumn 2022.

The values of the average concentrations of B, Cr, Ni, Cu, Zn, and As in the biocement were also normalized against the average seawater concentrations (Figure 6).

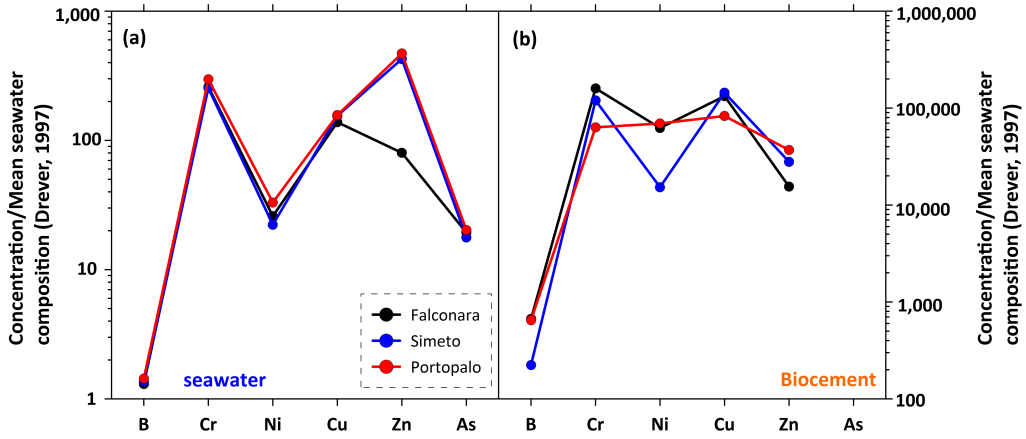

Figure 6. Mean seawater-normalized diagrams (data from [87]) of the concentrations of B, Cr, Ni, Cu, Zn, and As present in (**a**) seawater and (**b**) biocement sampled at the three sites.

A comparison of the normalized values in seawater and biocement (Figure 6a,b), despite the significantly higher ratios found in the solid fraction, showed a very good correlation between the different constituents. In the diagrams, comparable trends, characterized by positive peaks for Cr and Cu (and partly Zn) and negative peaks for B, Ni, and Zn, can be observed. These trends, in contrast to the findings for the major constituents, confirm a close dependence between the availability of trace elements (metals) in the formation area and subsequent bioaccumulation in the produced biocement.

4.3. Sabellariid Biocement as a New Environmental Proxy

The biocement is secreted in viscoelastic forms by the organisms but solidifies rapidly after contact with seawater and is thus in equilibrium with the external environment. In terms of biomineralization processes, it represents an intermediate product between controlled and influenced processes. Biomineralization is a generic term to indicate mineralization processes associated with biotic activity, and it has been studied extensively, mainly in carbonate rocks [93–95]. The formation of biominerals can be (i) controlled directly by organisms, such as in the skeletal formation of most organisms; (ii) induced by microbial communities by indirect precipitation mediated by their metabolic activities; or (iii) influenced by organic matter, with mineral formation on organic surfaces [96–104]. In all these cases, the formation of biominerals also depends on the chemical, physical, and climatic conditions of the environment [93,105]. These products are a direct marker of biological activity, and together with the soft tissues of the organisms, they are key elements in the study of the biological processes and past environmental conditions [106,107].

Recently, ref. [50] studied the bioaccumulation of trace metals in the tissues of polychaetes (*S. alveolata*), examining the relationships between the metal contents and physicochemical parameters of seawater. Their study revealed differences in the mean concentrations of trace metals (Fe > Al > Zn > Cu > Cd > Cr > Pb > Ag) between the investigated sites, seasons, and sites/season related to interactions between physical, chemical, and physiological factors. In their study, the authors found a positive correlation between Fe, Cu, and dissolved oxygen and a negative correlation between dissolved oxygen, Zn, and Al, indicating that a reduction in dissolved oxygen in the surrounding environment can promote the bioaccumulation of these two metals by *S. alveolata*. Furthermore, the authors defined a continental origin for elements such as Al and Fe (the same continental inputs) and an urban source for Cd, Cr, and Cu, while for Zn they hypothesized both origins. Their study demonstrated that most metals showed a seasonal trend of bioaccumulation, with high concentrations mainly in winter and summer. Bioaccumulation is therefore influenced

by interactions between physical (salinity, pH, temperature, etc.), chemical (metal concentration, speciation, etc.), and physiological factors linked to the organism itself ([50] and references therein). Regarding physical factors, the pH parameter is significantly affected by the presence of metals, as recorded by [108], who noted a negative correlation between pH and the contents of Cu, Pb, and Cr in Mytilus galloprovincialis on the Casablanca coastline (Atlantic coast of Morocco). This evidence was verified using data from actual mussels and was reported by [70,71], who stated that the availability of metals increases when the environment is alkaline, while it decreases when pH values are low. Indeed, a decrease in pH can increase the solubility of these metals and subsequently increase their accumulation in the skeletal fraction. Moreover, ref. [73] reported a positive correlation between the Zn bioaccumulated in the bivalve Lithophaga and the pH of seawater. As a result, the skeletal composition reflects that of the surrounding seawater, even if through their direct control the organisms may produce the mineral in disequilibrium with the medium of the water, thus representing an affordable environmental and paleo-environmental proxy.

Considering the organic nature of the sabellariid biocement, this component can be considered an "atypical" biomineralization product that reflects the double role of the organisms and the environment in its solidification. For this reason, we consider it a mutually controlled and influenced product that incorporates some trace elements in equilibrium with the surrounding seawater during the phase of solidification. This characteristic makes the sabellariid biocement a new affordable environmental and paleo-environmental proxy and a new tool for monitoring activities. The composition and morphology of most metazoan skeletons utilized thus far are directly controlled by the organisms and may not reflect the medium of the water in which the organisms live. Furthermore, as biocement is a solid component, it has a good possibility to be preserved in a subfossil state in the sedimentary environment and, different from the soft tissues that degrade quickly after the deaths of the organisms, may preserve the seawater chemical composition for hundreds or thousands of years.

4.4. Ecosystem Biodiversity

For its capability to build bioconstructions, *S. alveolata* can be considered an ecosystem engineer species capable of increasing the heterogeneity of primary substrates and creating a peculiar physical and biological habitat for a large variety of organisms [13,15,17,36,109,110]. These bioconstructions and the associated biota play key roles in ecosystem functioning, delivering services such as nutrient cycling, biofiltration, sediment trapping, and coastal erosion protection [19,26,111]. In the dynamic coastal system, *S. alveolata* reefs are highly vulnerable structures that undergo natural cycles of growth (progradation) and decline (retrogradation) [112], depending on a balance between biological and physical factors, such as recruitment of the *S. alveolata* larvae, competition with other invertebrates, the occurrence of epibionts, hydrodynamic forces, water temperature, and local environmental conditions [3,26,109,110,112]. In addition, the degradation of these fragile habitats, leading to serious impacts on biodiversity, has recently been a consequence of environmental perturbations due to direct or indirect anthropogenic pressures such as mechanical disturbances due to trampling and fishing as well as the organic enrichment and pollution of surrounding waters [13,15,19,35,36]. The study of the state of health of these bioconstructions is therefore a priority, and the search for new proxies aimed at understanding the relationship between bioconstructions and water chemistry goes in this direction.

5. Concluding Remarks

Geochemical analyses of the major constituents of the studied marine sites showed concentrations that were largely comparable to the mean seawater composition but with slight seasonal effects. The latter factor could be related to the greater evaporative effects characterizing the Mediterranean basin and the reduced input of fresh water from the main rivers during the prolonged summer period.

Geochemical analyses of trace elements of the three sites showed concentrations that were significantly higher than the mean seawater composition. The chemical variations observed during the different sampling periods were compared to the chemical compositional characteristics of the biocement to investigate the possible fractionation of perturbating elements (pollutants) on this bioproduct and the role played by the chemistry of the formation environment on the growth of the sabellariid bioconstructions. The comparison of the Ca/(Ca + Mg) ratio calculated using the average values of both the seawater and biocement from the three sites showed opposite trends between the ratios of the Ca and Mg concentrations of biocement and seawater from the same sites. The data showed that Ca and Mg are fractionated by biocement independent of the concentrations present in the formation environment, in contrast to the trace elements (Cr, Ni, Cu, Zn, and As), which showed good correlations.

Among the three sites, Falconara showed the lowest normalized average trace element values, while Simeto and Portopalo had the highest average values of Zn overall. This trend was also observed in the biocements, where the highest percentage of zinc was found in the samples from Simeto and Portopalo. These data indicate a correlation between the chemistry of the trace elements in biocement and that of the seawater. Such high values of Zn at all three sites suggest elevated environmental pollution caused by waste incineration as well as industrial and other wastewater. Water pollution due to heavy metals has been observed in coastal marine waters as a result of river, domestic, and industrial discharges.

The results of the geochemical studies highlight the importance of the environmental monitoring of waters to identify possible perturbations (pollution) that could affect the state of health of the complex and fragile habitats of *S. alveolata* and the associated biota.

Geochemical water analyses have been addressed for the first time to monitor their correspondence with the biocement of the biogenic reef in *S. alveolata*, a habitat considered "Data Deficient" by the European Red List of Habitats [37].

Even if further studies will be necessary to prove if the fractionation of pollutant elements (Cu, Zn, Cr, and Ni) in the biocement is in balance with the water concentration, the good correlation of the chemical composition between the waters and the biocement of *S. alveolata* suggests that the latter is a potential good proxy for environmental studies and is capable of recording short- and long-term variations in the geochemistry of the surrounding marine environment. This could be significant in the case of long-term variations recorded in the cement after its fossilization.

Author Contributions: A.G., R.S., C.D. and G.V. are the main authors and contributed to the scientific development of all parts of the research. Conceptualization, A.G. and R.S.; Methodology, A.G., R.S. and C.A.; Software, C.D., M.C. and G.V.; Validation, A.G., C.A. and R.S.; Formal Analysis, C.D., G.V., M.C., R.D. and D.B.; Investigation, C.D., G.V. and M.C.; Resources, A.G., R.S. and C.A.; Data Curation, C.D., M.C. and G.V.; Writing—original draft preparation, C.D., M.C. and G.V.; Writing—review and editing, A.G., R.S. and C.A.; Visualization, C.D., M.C. and G.V.; Supervision, A.G. and R.S.; Project Administration, A.G.; Funding Acquisition, A.G. and R.S. All authors have read and agreed to the published version of the manuscript.

Funding: This research was funded by MUR grants (ex 60% 2022 to A. Guido, University of Calabria).

Institutional Review Board Statement: Not applicable.

Informed Consent Statement: Not applicable.

Data Availability Statement: Not applicable.

Acknowledgments: The anonymous reviewers are thanked for their comments and fruitful suggestions for the preliminary version of the article. This is Catania Palaeoecological Research Group contribution No. 502.

Conflicts of Interest: The authors declare no conflict of interest.

References

1. Linnaeus, C. *Systema Naturae, per Regna Tria Naturae, Secundum Classes, Ordines, Genera, Species, Cum Caracteribus, Differentiis, Synonymis, Locis*; Editio duodecima, reformata; L. Salvii: Holmiae, Sweden, 1767; Volume I, Part 2; pp. 533–1327.
2. Vovelle, J. Le tube de *Sabellaria alveolata* (L.) Annelide Polychete Hermellidae et son ciment. Etude ecologique, experimentale, histologique et histochimique. *Arch. Zool. Exp. Gen.* **1965**, *106*, 1–187.
3. Gruet, Y.; Vovelle, J.; Grasset, M. Composante biominerale du ciment du tube ches *Sabellaria alveolata* (L.) Annelide Polychete. *Can. J. Zool.* **1987**, *65*, 837–842. [CrossRef]
4. Waite, J.H.; Jensen, R.A.; Morse, D.E. Cement precursor proteins of the reef–building polychaete *Phragmatopoma californica* (Fewkes). *Biochemistry* **1992**, *31*, 5733–5738. [CrossRef] [PubMed]
5. Zhao, H.; Sun, C.; Stewart, J.; Waite, J. Cement proteins of the tube–building polychaete *Phragmatopoma californica*. *J. Biol. Chem.* **2005**, *280*, 42938–42944. [CrossRef]
6. Gruet, Y. Aspects morphologiques et dynamiques de constructions de l'Annelide polychete *Sabellaria alveolata* (Linnaeus). *Rev. Trav. Inst. Peches Marit.* **1972**, *36*, 131–161.
7. Gruet, Y. Recherches sur l'écologie des" récifs" d'hermelles édifiés par l'Annélide Polychète *Sabellaria alveolata* (Linnaeus). Ph.D. Thesis, Université de Nantes, Nantes, France, 1982.
8. Naylor, L.A.; Viles, H.A. A temperate reef builder: An evaluation of the growth, morphology and composition of *Sabellaria alveolata* (L.) colonies on carbonate platforms in South Wales. *Geol. Soc. London Spéc. Publ.* **2000**, *178*, 9–19. [CrossRef]
9. Delbono, I.; Bianchi, C.N.; Morri, C. Le biocostruzioni di *Sabellaria alveolata* come indicatori ambientali: Area costiera fra Chiavari e Sestri Levante. In *Studi per la Creazione di Strumenti di Gestione costiera: Golfo del Tigullio*; Ferretti, O., Ed.; ENEA, Centro Ricerche Ambiente Marino: La Spezia, Italy, 2003; pp. 130–140.
10. Wilson, D. Sabellaria colonies at Duckpool, North Cornwall, 1961–1970. *J. Mar. Biol. Assoc. U. K.* **1971**, *51*, 509–580. [CrossRef]
11. Cunningham, P.N.; Hawkins, S.J.; Jones, H.D.; Burrows, M.T. The geographical distribution of *Sabellaria alveolata* (L.) in England, Wales and Scotland, with investigations into the community structure of, and the effects of trampling on *Sabellaria alveolata* colonies. In *Report to the Nature Conservancy Council from the Department of Zoology*; Manchester University: Manchester, UK, 1984; pp. 1–38.
12. Dias, A.S.; Paula, J. Associated fauna of *Sabellaria alveolata* colonies on the central coast of Portugal. *J. Mar. Biolog. Assoc.* **2001**, *80*, 169–170. [CrossRef]
13. Dubois, S.; Retière, C.; Olivier, F. Biodiversity associated with *Sabellaria alveolata* (Polychaeta: Sabellariidae) reefs: Effects of human disturbances. *J. Mar. Biol. Assoc. U. K.* **2002**, *82*, 817–826. [CrossRef]
14. Dubois, S.; Barille, L.; Retiere, C. Efficiency of particle retention and clearance rate in the polychaete Sabellaria alveolata L. *Comptes Rendus Biol.* **2003**, *326*, 413–421. [CrossRef]
15. Dubois, S.; Commito, J.A.; Olivier, F.; Retière, C. Effects of epibionts on *Sabellaria alveolata* (L.) biogenic reefs and their associated fauna in the Bay of Mont Saint–Michel. *Estuar. Coast. Shelf Sci.* **2006**, *68*, 635–646. [CrossRef]
16. Firth, L.B.; Mieszkowska, N.; Grant, L.M.; Bush, L.E.; Davies, A.J.; Frost, M.T.; Hawkins, S.J. Historical comparisons reveal multiple drivers of decadal change of an ecosystem engineer at the range edge. *Ecol. Evol.* **2015**, *5*, 3210–3222. [CrossRef]
17. Schlund, E.; Basuyaux, O.; Lecornu, B.; Pezy, J.P.; Baffreau, A.; Dauvin, J.C. Macrofauna associated with temporary *Sabellaria alveolata* reefs on the west coast of Cotentin (France). *SpringerPlus* **2016**, *5*, 1260. [CrossRef]
18. Holt, T.J.; Rees, E.I.; Hawkins, S.J.; Seed, R. Biogenic Reefs: An overview of dynamic and sensitivity characteristics for conservation management of marine SACs; UK Marine SACs Project. *Scott. Assoc. Mar. Sci.* **1998**, *IX*, 170.
19. Desroy, N.; Dubois, S.F.; Fournier, J.; Ricquiers, I.; Le Mao, P.; Guerine, L.; Gerla, D.; Rougerie, M.; Legendre, A. The conservation status of *Sabellaria alveolata* (L.) (Polychaeta: Sabellariidae) reefs in the Bay of Mont Saint Michel. *Aquat. Conserv. Mar. Freshw. Ecosyst.* **2011**, *21*, 462–471. [CrossRef]
20. Le Cam, J.B.; Fournier, J.; Etienne, S.; Couden, J. The strength of biogenic sand reefs: Visco–elastic behaviour of cement secreted by the tube building polychaete *Sabellaria alveolata*, Linnaeus, 1767. *Coast. Shelf Sci.* **2011**, *91*, 333–339. [CrossRef]
21. Nicoletti, L.; Lattanzi, L.; La Porta, B.; La Valle, P.; Gambi, M.C.; Tomassetti, P.; Chimenz Gusso, C. Biocostruzioni a Sabellaria delle coste del Lazio (Tirreno centrale). *Biol. Mar. Mediterr.* **2001**, *8*, 252–258.
22. La Porta, B.; La Valle, P.; Chimenz Gusso, C. *Sabellaria alveolata* (L.) (Polychaeta Sabellariidae): La selezione dei granuli di sedimento per la costruzione dei tubi. *Biol. Mar. Mediterr.* **2006**, *13*, 593–596.
23. Schimmenti, E.; Musco, L.; Lo Brutto, S.; Mikac, B.; Nygren, A.; Badalamenti, F. Mediterranean record of Eulalia ornata (Annelida: Phyllodocida) corroborating its fidelity link with the *Sabellaria alveolata* reef habitat. *Mediterr. Mar. Sci.* **2016**, *17*, 359–370. [CrossRef]
24. Bertocci, I.; Badalamenti, F.; Lo Brutto, S.; Mikac, B.; Pipitone, C.; Schimmenti, E.; Fernández, T.V.; Musco, L. Reducing the data–deficiency of threatened European habitats: Spatial variation of Sabellariid worm reefs and associated fauna in the Sicily Channel, Mediterranean Sea. *Mar. Environ. Res.* **2017**, *130*, 325–337. [CrossRef]
25. Sanfilippo, R.; Guido, A.; Insacco, G.; Deias, C.; Catania, G.; Reitano, A.; Leonardi, R.; Rosso, A. Distribution of *Sabellaria alveolata* (Polychaeta Sabellariidae) in the Mediterranean Sea: Update and new findings. *Zoosymposia* **2020**, *19*, 198–208. [CrossRef]
26. Bonifazi, A.; Lezzi, M.; Ventura, D.; Lisco, S.; Cardone, F.; Gravina, M.F. Macrofaunal biodiversity associated with different developmental phases of a threatened Mediterranean *Sabellaria alveolata* (Linnaeus, 1767) reef. *Mar. Environ. Res.* **2019**, *145*, 97–111. [CrossRef] [PubMed]

27. Borghese, J.; Arduini, D.; Schimmenti, E.; Iaciofano, D.; Mikac, B.; Badalamenti, F.; Giangrande, A.; Gravina, M.F.; Musco, L.; Lo Brutto, S. Assessment of the *Sabellaria alveolata* reefs' structural features along the Southern coast of Sicily (Strait of Sicily, Mediterranean Sea). *Mediterr. Mar. Sci.* **2022**, *23*, 890–899. [CrossRef]
28. Ingrosso, G.; Abbiati, M.; Badaloamenti, F.; Bavestrello, G.; Belmonte, G.; Cannas, R.; Benedetti-Cecchi, L.; Bertolino, M.; Bevilacqua, S.; Bianchi, C.N.; et al. Mediterranean Bioconstructions Along the Italian Coast. *Adv Mar Biol.* **2018**, *79*, 61–136.
29. Kirtley, D.W. Worm reefs as related to beach stabilization. *Shore Beach* **1967**, *35*, 31–34.
30. Bruschetti, M. Role of reef–building, ecosystem engineering polychaetes in shallow water ecosystems. *Diversity* **2019**, *11*, 168. [CrossRef]
31. Plicanti, A.; Domínguez, R.; Dubois, S.F.; Bertocci, I. Human impacts on biogenic habitats: Effects of experimental trampling on *Sabellaria alveolata* (Linnaeus, 1767) reefs. *J. Exp. Mar. Biol. Ecol.* **2016**, *478*, 34–44. [CrossRef]
32. Muller, R.A.; Stone, G.W. A climatology of tropical storm and hurricane strikes to enhance vulnerability prediction for the southeast U.S. coast. *J. Coast. Res.* **2001**, *17*, 949–956.
33. Wolff, N.H.; Wong, A.; Vitolo, R.; Stolberg, K.; Anthony, K.R.N.; Mumby, P.J. Temporal clustering of tropical cyclones on the Great Barrier Reef and its ecological importance. *Coral Reefs* **2016**, *35*, 613–623. [CrossRef]
34. Vorberg, R. Effects of shrimp fisheries on reefs of Sabellaria spinulosa (Polychaeta). *ICES J. Mar. Sci.* **2000**, *57*, 1416–1420. [CrossRef]
35. Plicanti, A.; Iaciofano, D.; Bertocci, I.; Lo Brutto, S. The amphipod assemblages of *Sabellaria alveolata* reefs from the NW coast of Portugal: An account of the present knowledge, new records, and some biogeographic considerations. *Mar. Biodivers.* **2016**, *47*, 521–534. [CrossRef]
36. Jones, A.G.; Dubois, S.F.; Desroy, N.; Fournier, J. Interplay between abiotic factors and species assemblages mediated by the ecosystem engineer *Sabellaria alveolata* (Annelida: Polychaeta). *Estuar. Coast. Shelf Sci.* **2018**, *200*, 1–18. [CrossRef]
37. Gubbay, S.; Sanders, N.; Haynes, T.; Janssen, J.R.; Rodwell, J.A.M.; Nieto, M.; García Criado, M.; Beal, S.; Borg, J.; Kennedy, M.; et al. *European Red List of Habitats. Marine Habitats*; European Union Publication Offices: Luxembourg, 2016; Volume 1, p. 48.
38. Coclet, C.; Garnier, C.; D'Onofrio, S.; Durrieu, G.; Pasero, E.; Le Poupon, C.; Omanović, D.; Mullot, J.U.; Misson, B.; Briand, J.F. Trace metal contamination impacts predicted functions more than structure of marine prokaryotic biofilm communities in an anthropized coastal area. *Front. Microbiol.* **2021**, *12*, 589948. [CrossRef]
39. Little, C.; Williams, G.A.; Trowbridge, C.D. *The Biology of Rocky Shores*; Oxford University Press: Oxford, England, 2009; p. 376.
40. Gillet, P. Bioaccumulation du cuivre et du zinc chez Nereis diversicolor (Annélide Polychète) de l'estuaire du Bou Regreg (Maroc). *Cah. Biol. Mar.* **1987**, *28*, 339–350.
41. Cheggour, M.; Texier, H.; Moguedet, G.; Elkaïm, B. Metal exchange in the fauna–sediment system. The case of Nereis diversicolor and Scrobicularia plana in the Bou Regreg estuary (Morocco). *Hydrobiologia* **1990**, *207*, 209–219. [CrossRef]
42. Ait Alla, A.; Gillet, P.; Deutsch, B.; Moukrim, A.; Bergayou, H. Response of Nereis diversicolor (Polychaeta, Nereididae) populations to reduced wastewater discharge in the polluted estuary of Oued Souss, Bay of Agadir, Morocco Estuar. *Coast. Shelf Sci.* **2006**, *70*, 633–642. [CrossRef]
43. Ferssiwi, A. Accumulation du Cadmium, Cuivre et zinc dans le Sédiment et chez Quatre espèces D'annélides Polychètes du Littoral d'El Jadida (Côte Atlantique Marocaine): Implication des Proteins Type Metallothioneines. Ph.D. Thesis, University of Chouaïb Doukkali, El Jadida, Morocco, 2007.
44. Dean, H.K. The use of polychaetes (Annelida) as indicator species of marine pollution: A review. *Rev. Biol. Trop.* **2008**, *56*, 11–38.
45. Rouhi, A.; Sif, J.; Chemaa, A. Evaluation de la pollution métallique du littoral de la ville d'El Jadida (Maroc) utilisation de l'annélide Arenicola grubii comme indicateur biologique. *Bull. Inst. Sci. Rabat. Sect. Sci. Vie.* **2012**, *34*, 163–171.
46. Idardare, Z.; Moukrim, A.; Chiffoleau, J.F.; Ait Alla, A.; Auger, D.; Rozuel, E. Evaluation de la contamination métallique dans deux lagunes marocaines: Khnifiss et Oualidia. *Rev. Mar. Sci. Agron. Vét.* **2013**, *2*, 58–67.
47. Pini, J.M.; Richir, J.; Watson, G.J. Metal bioavailability and bioaccumulation in the polychaete Nereis (Alitta) virens (Sars): The effects of site–specific sediment characteristics. *Mar. Pollut. Bull.* **2015**, *95*, 565–575. [CrossRef]
48. Rouhi, A.; Sif, J.; Ferssiwi, A.; Chemaa, A. Bioaccumulation de quelques éléments métalliques par deux espèces d'Annélides Polychètes du littoral de Jorf Lasfar (Région d'El Jadida, Maroc). *Bull. Inst. Sci. Rabat. Sect. Sci. Vie.* **2007**, *29*, 81–87.
49. Chouikh, N.; Gillet, P.; Langston, W.J.; Cheggour, M.; Maarouf, A.; El Hachimi, Y.; Mouabad, A. Spatial and temporal assessment of metals contamination in the surface sediments of biogenic intertidal reefs of *Sabellaria alveolata* (Annelida: Polychaeta) from Essaouira protected coastal area (Atlantic coast of Morocco). *Reg. Stud. Mar. Sci.* **2021**, *48*, 101998. [CrossRef]
50. Chouikh, N.; Gillet, P.; Cheggour, M.; Maarouf, A.; EL Hachimi, Y.; Mounir, A.; Alahyane, H.; Mouabad, A. Bioaccumulation of trace metals in *Sabellaria alveolata* (Annelida: Polychaeta) and their controlling factors along the Essaouira Protected Coastal Area (Atlantic Coast of Morocco). *Ocean Sci. J.* **2022**, *57*, 224–238. [CrossRef]
51. Flammang, P.; Lambert, A. Cement ultrastructure and adhesive glands morphology in the tube–dwelling polychaete *Sabellaria alveolata*. *J. Morphol.* **2008**, *269*, 1479–11479.
52. Fournier, J.; Etienne, S.; Le Cam, J.B. Inter– and intraspecific variability in the chemical composition of the mineral phase of cements from several tube–building polychaetes. *Geobios* **2010**, *43*, 191–200. [CrossRef]
53. Sanfilippo, R.; Rosso, A.; Mastandrea, A.; Viola, A.; Deias, C.; Guido, A. *Sabellaria alveolata* sandcastle worm from the Mediterranean Sea: New insights on tube architecture and biocement. *J. Morphol.* **2019**, *280*, 1839–1849. [CrossRef]
54. Stewart, R.J.; Weaver, J.C.; Morse, D.E.; Waite, J.H. The tube cement of *Phragmatopoma californica*: A solid foam. *J. Exp. Biol.* **2004**, *207*, 4727–4734. [CrossRef]

55. Stewart, R.J.; Wang, C.S.; Song, I.T.; Jones, J.P. The role of coacervation and phase transitions in the sandcastle worm adhesive system. *Adv. J. Colloid Interface Sci.* **2017**, *239*, 88–96. [CrossRef]
56. Stevens, M.J.; Steren, R.E.; Hlady, V.; Stewart, R.J. Multiscale structure of the underwater adhesive of *Phragmatopoma californica*: A nanostructured latex with a steep microporosity gradient. *Langmuir* **2007**, *23*, 5045–5049. [CrossRef]
57. Sun, C.J.; Fantner, G.E.; Adams, J.; Hansma, P.K.; Waite, J.H. The role of calcium and magnesium in the concrete tubes of the sandcastle worm. *J. Exp. Biol.* **2007**, *210*, 1481–1488. [CrossRef]
58. Wang, C.S.; Svendsen, K.K.; Stewart, R.J. Morphology of the adhesive system in the sandcastle worm, *Phragmatopoma californica*. In *Biological Adhesive Systems: From Nature to Technical and Medical Applications*; von Byern, J., Grunwald, I., Eds.; Springer: Wien, NY, USA, 2010; pp. 1–11.
59. Wang, C.S.; Stewart, R.J. Localization of the bioadhesive precursors of the sandcastle worm, *Phragmatopoma californica* (Fewkes). *J. Exp. Biol.* **2012**, *215*, 351–361. [CrossRef]
60. Langston, W.J.; Spence, S.K. Biological factors involved in metal concentrations observed in aquatic organisms. In *Metal Speciation and Bioavailability in Aquatic System*; IU–PAC; Teissier, A., Turner, D.R., Eds.; John Wiley and Sons: Chichester, UK; London, UK, 1995; Volume 3, pp. 407–478.
61. Batten, S.D.; Bamber, R.N. The effects of acidified seawater on the polychaete Nereis virens (Sars, 1835). *Mar. Pollut. Bull.* **1996**, *32*, 283–287. [CrossRef]
62. Amiard, J.C.; Geffard, A.; Amiard–Triquet, C. La métallothionéine chez la moule *Mytilus edulis* comme biomarqueur de pollution métallique: Variabilité entre sites, saisons et organes. *J. Rech. Oceangr.* **1998**, *23*, 25–30.
63. Fattorini, D.; Notti, A.; Di Mento, R.; Cicero, A.M.; Gabellini, M.; Russo, A.; Regoli, F. Seasonal, spatial and inter–annual variations of trace metals in mussels from the Adriatic Sea: A regional gradient for arsenic and implications for monitoring the impact of offshore activities. *Chemosphere* **2008**, *72*, 1524–1533. [CrossRef]
64. Coccioni, R.; Frontalini, F.; Marsili, A.; Mana, D. Benthic foraminifera and trace element distribution: A case–study from the heavily polluted lagoon of Venice (Italy). *Mar. Pollut. Bull.* **2009**, *59*, 257–267. [CrossRef]
65. Frontalini, F.; Coccioni, R.; Bucci, C. Benthic foraminiferal assemblages and trace element contents from the lagoons of Orbetello and Lesina. *Environ. Monit. Assess.* **2010**, *170*, 245–260. [CrossRef]
66. Stanković, S.; Jović, M.; Stanković, A.R.; Katsikas, L. Heavy metals in seafood mussels. Risks for human health. In *Environmental Chemistry for A Sustainable World*; nanotechnology and health risk; Lichtfouse, E., Schwarzbauer, J., Robert, D., Eds.; Springer: Dordrecht, The Netherlands; Heidelberg, Germany; London, UK; New York, NY, USA, 2012; Volume 1, pp. 311–373.
67. Perošević, A.; Pezo, L.; Joksimović, D.; Đurović, D.; Milašević, I.; Radomirović, M.; Stanković, S. The impacts of seawater physicochemical parameters and sediment metal contents on trace metal concentrations in mussels—A chemometric approach. *Environ. Sci. Pollut. Res.* **2018**, *25*, 28248–28263. [CrossRef]
68. Karbe, L.; Antonacopoulos, N.; Schnier, C. The influence of water quality on accumulation of heavy metals in aquatic organisms. *SIL Proc.* **1975**, *19*, 2094–2101. [CrossRef]
69. Lea, D.W. Trace elements in foraminiferal calcite. In *Modern Foraminifera*; Springer: Dordrecht, The Netherlands, 1999; pp. 259–277.
70. Lemaire, N. Variations saisonnières de paramètres physiologiques chez la moule bleue *Mytilus* spp. dans différents sites d'élevage mytilicole de l'Est du Québec. Master's Thesis, University of Québec, Rimouski, QC, Canada, 2005.
71. Lemaire, N.; Pellerin, J.; Fournier, M.; Girault, L.; Tamigneaux, E.; Cartier, S.; Pelletier, E. Seasonal variations of physiological parameters in the blue mussel Mytilus spp. from farm sites of eastern Quebec. *Aquaculture* **2006**, *261*, 729–751. [CrossRef]
72. Jitar, O.; Teodosiu, C.; Oros, A.; Plavan, G.; Nicoara, M. Bioaccumulation of heavy metals in marine organisms from the Romanian sector of the Black Sea. *N. Biotechnol.* **2015**, *32*, 369–378. [CrossRef]
73. Kefi, J.J.; Mleiki, A.; Béjaoui, J.M.; El Menif, N.T. Seasonal variations of trace metal concentrations in the soft tissue of Lithophaga lithophaga collected from the Bizerte bay (Northern Tunisia, Mediterranean Sea). *J. Aquac. Res. Dev.* **2016**, *7*, 432.
74. Marchitto, T.M.; Demenocal, P.B. Late Holocene variability of upper North Atlantic Deep Water temperature and salinity. *Geochem. Geophys. Geosystems* **2003**, *4*, 1100. [CrossRef]
75. McGann, M. High–Resolution foraminiferal, isotopic, and trace element records from Holocene estuarine deposits of San Francisco Bay, California. *J. Coast. Res.* **2008**, *24*, 1092–1109. [CrossRef]
76. Kocsis, L. Geochemical compositions of marine fossils as proxies for reconstructing ancient environmental conditions. *Chimia* **2011**, *65*, 787–791. [CrossRef]
77. Grasso, M.; Licorish, W.H.; Diliberto, S.E.; Geremia, F.; Maniscalco, R.; Maugeri, S.; Pappalardo, G.; Rapisarda, F.; Scamarda, G. *Geological Map of the Licata fold belt (South Central Sicily): Explanatory Notes*; Annales Tectonicae: Firenze, Italy, 1998; Volume XII, pp. 51–58.
78. Longhitano, S. Sedimentary features of incipient beachrock deposits along the coast of Simeto river delta (eastern Sicily, Italy). *GeoActa* **2003**, *1*, 99–113.
79. Longhitano, S.; Colella, A. Geomorphology, sedimentology and recent evolution of the anthropogenically modified Simeto River delta system (eastern Sicily, Italy). *Sediment. Geol.* **2007**, *194*, 195–221. [CrossRef]
80. Di Stefano, A.; De Pietro, R.; Monaco, C.; Zanini, A. Anthropogenic influence on coastal evolution: A case history from the Catania Gulf shoreline (eastern Sicily, Italy). *Ocean Coast. Manag.* **2013**, *80*, 133–148. [CrossRef]
81. Lentini, F.; Carbone, S. *Geologia della Sicilia–Geology of Sicily*; Carta Geologica d'Italia: Roma, Italy, 2014; Volume 95, pp. 7–414.
82. Sanfilippo, R.; Serio, D.; Deias, C.; Rosso, A. *Sabellaria alveolata* (Annelida, Polychaeta) bioconstructions and associated macroalgal community from Portopalo di Capo Passero (SE Sicily). *Mediterr. Mar. Sci.* **2022**, *23*, 150–156. [CrossRef]

83. PAI. *Piano Stralcio di Bacino per L'assetto Idrogeologico Della Regione Siciliana*; Assessorato Territorio e Ambiente, Regione Sicilia: Palermo, Italy, 2004; p. 176.
84. Martino, C.; Di Stefano, A.; Monaco, C.; Zanini, A.; Curcuruto, E.P. Fenomeni erosivi lungo il litorale di Marina di Butera (CL), Sicilia centro–meridionale. *Geol. di Sicil.* **2011**, *3*, 4–15.
85. Borzì, L.; Anfuso, G.; Manno, G.; Distefano, S.; Urso, S.; Chiarella, D.; Di Stefano, A. Shoreline Evolution and Environmental Changes at the NW Area of the Gulf of Gela (Sicily, Italy). *Land* **2021**, *10*, 1034. [CrossRef]
86. Nordstrom, D.K. Thermochemical redox equilibria of ZoBell's solution. *Geochim. Cosmochim. Acta* **1977**, *41*, 1835–1841. [CrossRef]
87. Drever, J.I. *The Geochemistry of Natural Waters*; Prentice Hall, Inc.: Englewood Cliffs, NJ, USA, 1988.
88. Randazzo, P.; Caracaus, A.; Aiuppa, A.; Cardellini, C.; Chiodini, G.; Apollaro, C.; Paternoster, M.; Rosiello, A.; Vespasiano, G. Active degassing of crustal CO_2 in areas of tectonic collision: A case study from the Pollino and Calabria sectors (Southern Italy). *Front. Earth Sci.* **2022**, *10*, 1–18. [CrossRef]
89. Vespasiano, G.; Marini, L.; Muto, F.; Auqué, L.F.; Cipriani, M.; De Rosa, R.; Critelli, S.; Gimeno, M.J.; Blasco, M.; Dotsika, E.; et al. Chemical, isotopic and geotectonic relations of the warm and cold waters of the Cotronei (Ponte Coniglio), Bruciarello and Repole thermal areas, (Calabria—Southern Italy). *Geothermics* **2021**, *96*, 102228. [CrossRef]
90. Nisi, B.; Vaselli, O.; Elio, J.; Giannini, L.; Tassi, F.; Guidi, M.; Darrah, T.H.; Maletic, E.L.; Delgado Huertas, A.; Marchionni, S. The Campo de Calatrava Volcanic Field (central Spain): Fluid geochemistry in a CO_2–rich area. *Appl. Geochem.* **2019**, *102*, 153–170. [CrossRef]
91. Vespasiano, G.; Cianflone, G.; Marini, L.; De Rosa, R.; Polemio, M.; Walraevens, K.; Vaselli, O.; Pizzino, L.; Cinti, D.; Capecchiacci, F.; et al. Hydrogeochemical and isotopic characterization of the Gioia Tauro coastal Plain (Calabria–southern Italy): A multidisciplinary approach for a focused management of vulnerable strategic systems. *Sci. Total Environ.* **2023**, *862*, 160694. [CrossRef]
92. Apollaro, C.; Tripodi, V.; Vespasiano, G.; De Rosa, R.; Dotsika, E.; Fuoco, I.; Critelli, S.; Muto, F. Chemical, isotopic and geotectonic relations of the warm and cold waters of the Galatro and Antonimina thermal areas, southern Calabria, Italy. *Mar. Pet. Geo.* **2019**, *109*, 469–483. [CrossRef]
93. Riding, R. Microbialites, stromatolites, and thrombolites. In *Encyclopedia of Geobiology*; Reitner, J., Thiel, V., Eds.; Encyclopedia of Earth Science Series; Springer: Heidelberg, Germany, 2011; pp. 635–654.
94. Riding, R. Microbial carbonates: The geological record of calcified bacterial-algal mats and biofilms. *Sedimentology* **2000**, *47*, 179–214. [CrossRef]
95. Van Driessche, A.E.S.; Stawski, T.M.; Kellermeier, M. Calcium sulfate precipitation pathways in natural and engineered environments. *Chem. Geol.* **2019**, *530*, 119274. [CrossRef]
96. Lowenstam, H.A.; Weiner, S. *On Biomineralization*; Oxford University Press: New York, NY, USA, 1989.
97. Mastandrea, A.; Barca, D.; Guido, A.; Tosti, F.; Russo, F. Rare earth element signatures in the Messinian pre-evaporitic Calcare di Base formation (Northern Calabria, Italy): Evidence of normal seawater deposition. *Carbonates Evaporites* **2010**, *25*, 133–143. [CrossRef]
98. Benzerara, K.; Miot, J.; Morin, G.; Ona-Nguema, G.; Skouri-Panet, F.; Ferard, C. Significance, mechanisms and environmental implications of microbial biomineralization. *CR Geosci.* **2011**, *343*, 160–167. [CrossRef]
99. Phillips, A.J.; Gerlach, R.; Lauchnor, E.; Mitchell, A.C.; Cunningham, A.B.; Spangler, L. Engineered applications of ureolytic biomineralization: A review. *Biofouling* **2013**, *29*, 715–733. [CrossRef] [PubMed]
100. Anbu, P.; Kang, C.H.; Shin, Y.J.; So, J.S. Formations of calcium carbonate minerals by bacteria and its multiple applications. *SpringerPlus* **2016**, *5*, 250. [CrossRef] [PubMed]
101. Riding, R.; Virgone, A. Hybrid Carbonates: In situ abiotic, microbial and skeletal coprecipitates. *Earth Sci. Rev.* **2020**, *208*, 103300. [CrossRef]
102. Guido, A.; Gerovasileiou, V.; Russo, F.; Rosso, A.; Sanfilippo, R.; Voultsiadou, E.; Mastandrea, A. Composition and biostratinomy of sponge-rich biogenic crusts in sub marine caves (Aegean Sea, Eastern Mediterranean). *Palaeogeogr. Palaeoclimatol. Palaeoecol.* **2019**, *534*, 109338. [CrossRef]
103. Guido, A.; Mastandrea, A.; Rosso, A.; Sanfilippo, R.; Russo, F. Micrite precipitation induced by sulphate reducing bacteria in serpulid bioconstructions from submarine caves (Syracuse, Sicily). *Rend. Online Soc. Geol. Ital.* **2012**, *21*, 933–934.
104. Guido, A.; Sposato, M.; Palladino, G.; Vescogni, A.; Miriello, D. Biomineralization of primary carbonate cements: A new biosignature in the fossil record from the Anisian of Southern Italy. *Lethaia* **2022**, *55*, 1–21. [CrossRef]
105. Riding, R.; Liang, L. Geobiology of microbial carbonates: Metazoan and seawater saturation state influences on secular trends during the Phanerozoic. *Palaeogeogr. Palaeoclimatol. Palaeoecol.* **2005**, *219*, 101–115. [CrossRef]
106. Guido, A.; Rosso, A.; Sanfilippo, R.; Russo, F.; Mastandrea, A. Microbial biomineralization in biotic crusts from a Pleistocene marine cave (NW Sicily, Italy). *Geomicrobiol. J.* **2017**, *34*, 864–872. [CrossRef]
107. Guido, A.; Rosso, A.; Sanfilippo, R.; Miriello, D.; Belmonte, G. Skeletal vs microbialite geobiological role in bioconstructions of confined marine environments. *Palaeogeogr. Palaeoclimatol. Palaeoecol.* **2022**, *593*, 110920. [CrossRef]
108. Bouthir, F.Z.; Chafik, A.; Benbrahim, S.; Souabi, S.; El Merdhy, H.; Messoudi, A. Qualité physico–chimique des eaux côtières du littoral de la Wilaya du grand Casablanca (océan Atlantique marocain) utilisant la moule Mytilus galloprovincialis comme indicateur de la contamination métallique. *Mar. life* **2004**, *14*, 59–70.
109. Cole, V.J.; Chapman, M.G.; Underwood, A.J. Landscapes and life-histories influence colonisation of polychaetes to intertidal biogenic habitats. *J. Exp. Mar. Biol. Ecol.* **2007**, *348*, 191–199. [CrossRef]
110. La Porta, B.; Nicoletti, L. *Sabellaria alveolata* (Linnaeus) reefs in the central Tyrrhenian Sea (Italy) and associated polychaete fauna. *Zoosymposia* **2009**, *2*, 527–536. [CrossRef]

111. Gravina, M.F.; Cardone, F.; Bonifazi, A.; Bertrandino, M.S.; Chimienti, G.; Longo, C.; Marzano, C.N.; Moretti, M.; Lisco, S.; Moretti, V.; et al. Sabellaria spinulosa (Polychaeta, Annelida) reefs in the Mediterranean Sea: Habitat mapping, dynamics and associated fauna for conservation management. *Estuar. Coast. Shelf Sci.* **2018**, *200*, 248–257. [CrossRef]
112. Curd, A.; Fabrice Pernet, F.; Corporeau, C.; Delisl, L.; Firt, L.B.; Nunes, F.L.D.; Dubois, S. Connecting organic to mineral: How the physiological state of an ecosystem-engineer is linked to its habitat structure. *Ecol. Indic.* **2019**, *98*, 49–60. [CrossRef]